Supporting Information

Selective Binding of Sulphated Glycosaminoglycan Induces Self-Assembly of Naphthalene Diimide into Fluorescent Nanofibers

Poonam Sharma,[a,e] Esteban Fernández-Pedrera López,[a] Beatriz Cantero Nieto,[b] Annalisa Calò[b,c,d] Subhadip Ghosh,[b] Paula Rodríguez,[a] Xavier Companyó,[a] Bart Limburg,[a,e] and Mohit Kumar*[a,b,e]

[a]*Department of Inorganic and Organic Chemistry, University of Barcelona, Calle Marti i Fraquès 1-11, 08028 Barcelona (Spain). Email: mohit.kumar@ub.edu*

[b]*Institute for Bioengineering of Catalonia (IBEC), Calle Baldiri Reixac 10–12, 08028 Barcelona (Spain)*

[c]*Department of Electronic and Biomedical Engineering, University of Barcelona, Calle Marti i Fraquès 1-11, 08028 Barcelona (Spain)*

[d]*Institute of Nanoscience and Nanotechnology, University of Barcelona, 08028 Barcelona (Spain)*

[e]*Institut de Quìmica Teòrica i Computacional, University of Barcelona, 08028 Barcelona (Spain*

Table of Contents

1. Materials and methods

All reagents used were commercially sourced and used as received unless otherwise specified. Dichloromethane, DMF, DMSO and acetonitrile was obtained from PanReac Química S.L.U., Thermo Fisher Scientific, S.L. and Merck Sigma. Naphthalene-1,4,5,8-tetracarboxylic dianhydride (NDA) was also obtained from Merck Sigma. Decylamine and N,N-Dimethylethylenediamine were purchased from Thermo Fisher Scientific, S.L. and Merck Sigma. Heparin sodium salt derived from porcine intestinal mucosa was purchased from Thermo Fisher Scientific, S.L.

Stock Solution preparation

For all measurements, stock solution of derivative **1** was prepared in acetonitrile and DMSO (5 mM). The working concentration of all samples was 50 µM in different DMSO-water and acetonitrile-water ratios. The same method was followed for the compound **2**. The stock solution of compound **3** was prepared at a concentration of 1 mM in acetonitrile, and the working concentration was 50 µM.

Heparin stock solution of 25.8 mg/ml was prepared by dissolving 5.16 mg in 200 µL milli-Q water. We calculated the effective molecular weight of monosaccharide unit of heparin and used this value to add heparin that is in the same order of concentration (in

molarity) as that of NDI. The molecular weight of monosaccharide was approximated to be 258 gms per mole and based on that we added 1 to 10 molar equivalents (50 to 500 μM) of monosaccharide w.r.t. the concentration of NDI. This is indeed an approximation of the monosaccharide molecular weight as the heparin structure contains different monosaccharide units.

NMR

The ^{1}H and ^{13}C NMR spectra were recorded on Bruker 400 spectrometer at room temperature using $CDCl_3$ and DMSO-*d*$_6$ as a solvent. Chemical shift (δ) values are reported in parts per million (ppm). Solvent peaks appear at δ 2.50 for DMSO-*d*$_6$ and δ 7.26 for $CDCl_3$, while in ^{13}C NMR, the DMSO solvent peak appears at δ 39.52. ^{1}H NMR spectra provide details on chemical shifts, integration, multiplicity, and signal assignments, using abbreviations such as s (singlet), d (doublet), t (triplet), q (quartet), and m (multiplet). ^{1}H NMR titrations of **1** with heparin were performed using concentration of 0.5 mM as lower concentrations were unable to produce reliable NMR signal.

UHPLC-MS

UHPLC-MS measurements were obtained with Acquity Arc FTN-R instrument equipped with 2998 photodiode array (PDA) UV detector by Waters Corporation and the MS was performed using electrospray ionization (ESI+).

UV-Visible absorption spectroscopy

2.5 ml samples were placed in a glass cuvette of 10 mm path length to measure the UV-Visible absorbance spectra with an Agilent Cary 5000 spectrophotometer at a scanning speed of 600 nm per minute. The spectra were recorded in the range of 300-550 nm.

Fluorescence spectroscopy

2.5 ml samples were placed in glass cuvettes of 10 mm path length to measure the fluorescence spectra using Photon Technology International (PTI) fluorometer which uses a xenon arc lamp light source. The excitation wavelength was set at 330 nm.

Time-Correlated Single Photon Counting (TCSPC)

Time-correlated Single Photon Counting experiments were performed with an Edinburgh Instruments FS-5 fluorimeter equiped with an EPL-405 picosecond diode laser (excitation at 401.6 nm). Lifetime data were collected in 1024 channels at 5000 peak counts and fitted using a reconvolution fit procedure using an instrument response function collected by measuring scattered laser light at 401.6 nm right after the experiment was run.

Cyclic Voltammetry (CV): Cyclic voltammetry measurements were carried out with a computer-controlled potentiostat Model Epsilon EClipse (BASi) with 10 and 100 mV/s. The setup comprises an undivided cell, a glassy carbon working electrode (3 mm diameter), a platinum wire counter electrode, and a saturated Ag/AgCl reference electrode. All samples at a working concentration of 100 μM were previously purged

under N_2 to avoid the presence of oxygen during the measurements. The measurements were performed without any supporting electrolyte as the supporting electrolyte could affect the strength of heparin binding to NDIs.

Atomic Force Microscopy (AFM)

Atomic force microscopy (AFM) measurements were performed using a NanoWizard 4 BioScience AFM (JPK Instruments, Bruker) operated in tapping mode (AC mode). Commercial silicon cantilevers (PPP-CONTR, NanoSensors) with a spring constant of 0.36 $N \cdot m^{-1}$, determined by thermal noise method, were used throughout the study. Prior to imaging, the cantilever was tuned to its resonance frequency (16 kHz), and oscillation parameters were optimized to ensure stable tapping conditions. The sensitivity of the system was obtained from the slope of the linear region of the force–distance curve recorded on a hard surface, allowing conversion of the deflection signal from volts to nanometers.

Topographical images were acquired over 4 × 4 μm^2 and 1.2 × 1.2 μm^2 scan areas (400 × 400 pixels) at a line rate of 0.70 Hz. The free oscillation amplitude was 55.72 nm, whereas the setpoint amplitude was fixed at 20.2 nm, ensuring a low-interaction imaging regime. The feedback loop was operated using integral and proportional gains (I_{Gain}/P_{Gain}) of 400.0Hz and 0.0064, respectively. All measurements were carried out in air at room temperature.

AFM data were processed and leveled using the JPK Data Processing software.

Samples for AFM analysis were prepared in 70% H_2O in acetonitrile solvent composition. For sample deposition, 50 µL of the solution was drop-cast onto the freshly cleaved mica and allowed to spread under ambient conditions. Deposited films were dried in air for 2–3 h, after which they were stored in a desiccator for 24 h to ensure complete solvent removal.

Transmission Electron microscopy (TEM)

The TEM images were recorded on TEM microscope: JEOL JEM 1010 80kV microscope operating at an accelerating voltage of 80 kV. The samples for TEM analysis were prepared by drop casting 5 µL aliquot of the sample solution on a carbon film grid (400 mesh, copper) and dried completely over the grid for 1 hour. Then, 5 µL uranyl acetate stain (2% solution) was drop cast, blotted away after 30 seconds, and then dried completely. Then grid was dried overnight under high vacuum before imaging.

Confocal Laser Scanning Microscopy (CLSM)

For fluorescence imaging, 5 µL of the sample solution was sandwiched between two glass cover slips. The imaging was performed on a Zeiss LSM800 confocal fluorescence microscope using a 63x oil-immersion objective and a PMT detector. The samples were excited with 405 nm diode lasers and the emission was collected over 500-700 nm. Images were recorded at 25°C at a resolution of 1024×1024 pixels. Fiji ImageJ software was used for image processing.

Binding affinity

The binding affinity or association constant in Figure S19 was obtained with GraphPad Prism 10 using the non-linear regression analysis model i.e. allosteric binding model.

2. Synthesis

Molecule 1 was synthesized according to Scheme S1.

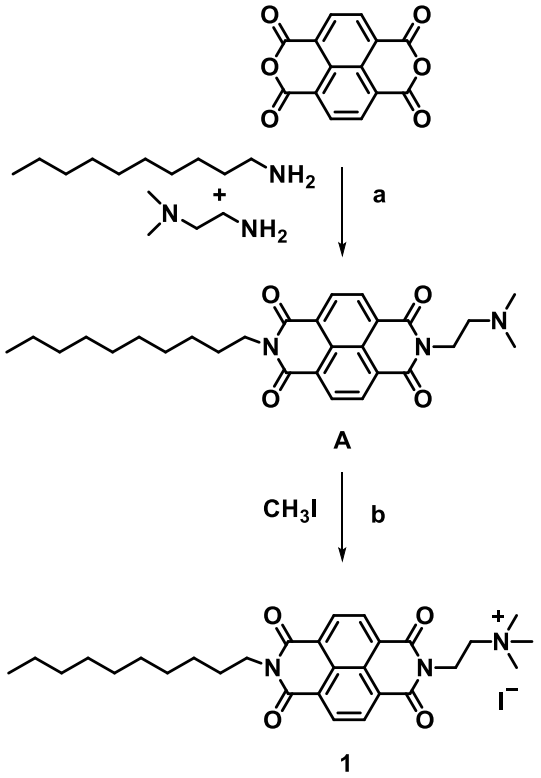

Scheme S1: Synthetic Outline of the **1**. (a) Dry DMF, 100°C, N_2, 12h; (b) CH_3I, 45°C, 4h.

Synthetic procedures:

Synthesis of A:

N, N-dimethylethylenediamine (345 µL, 3.92 mmol) and decylamine (647 µL, 3.92 mmol) were dissolved in dry DMF (50 mL). Then 1,4,5,8-Naphthalenetetracarboxylic dianhydride (1 g, 3.73 mmol) was added to the reaction mixture. After that the reaction mixture was stirred for 12h at 100°C under N_2 atmosphere. The progress of the reaction was monitored using TLC. After reaction completion, DMF was evaporated under high vacuum on a rotary evaporator to get crude product. It was further purified by column chromatography using silica gel and EtOAc/Hexane (60/40, v/v) as an eluent to get the pure product.

After column, the sample still contained some impurity of NDI with both sides decyl chain, the unwanted side product of the reaction. This sample contained 92% of A as confirmed by NMR. We used it as it is for the next step of the reaction expecting an easy purification process in the next step. This is because the impurity was soluble in toluene

and was expected to be unreactive towards methyl iodide of the next step. So, it was easier to remove it in the next step to get pure product **1**.

^{1}H NMR (400 MHz, $CDCl_3$) δ 8.75 (s, 4H), 4.35 (t, J = 8.0 Hz, 2H), 4.19 (t, J = 8.0 Hz, 2H), 2.67 (t, J = 8.0 Hz, 2H), 2.34 (s, 6H), 1.78– 1.70 (m, 2H), 1.46– 1.25 (m, 14H), 0.87 (t, 8.0 Hz, 3H). The NMR integration value was not matching the theoretically expected value because of the presence of impurity as described above (Figure S1). ESI-MS: m/z calc for $C_{28}H_{35}N_3O_4$: $[M+H]^+$: 478.27; found: 478.3 $[M+H]^+$ (Figure S2).

Synthesis of **1**:

In a 50 mL round-bottom flask equipped with a magnetic sir bar, A (150 mg, 0.514 mmol, 1 equiv.) was dissolved in 7 mL toluene. To this stirring solution, methyl iodide (390 µL, 6.28 mmol, 20 equiv.) was slowly added using a glass syringe. The reaction mixture was heated at 45°C for 4 h. After the completion of the reaction, the solution was allowed to cool. Then it was filtered and washed with Et_2O (3×10 mL) to remove all the impurities. Finally, the pure product was dried, yielding 100 mg of red solid in 51% yield. ^{1}H NMR (400 MHz, DMSO-*d*$_6$) δ 8.69 (s, 4H), 4.48 (t, J = 8.0 Hz, 2H), 4.04 (t, J = 8.0 Hz, 2H), 3.64 (t, J = 8.0 Hz, 2H), 3.23 (s, 9H), 1.70– 1.60 (m, 2H), 1.48– 1.17 (m, 14H), 0.84 (t, J = 8.0 Hz, 3H). δ ^{13}C NMR (DMSO-*d*$_6$, 100 MHz) δ 162.8, 162.6, 130.6, 130.5, 126.6, 126.3, 126.2, 61.7, 52.5, 33.9, 31.3, 29.0, 28.9, 28.7, 28.7, 27.4, 26.5, 22.1, 14.0. ESI-MS: m/z calc for $C_{29}H_{38}N_3O_4^+$: $[M^+]$: 492.64; found: 492.3 $[M^+]$ (Figure S3-5).

Control molecules 2 and 3 were synthesized according to the reported procedures[1] and were accordingly characterized.

3. Supplementary Figures

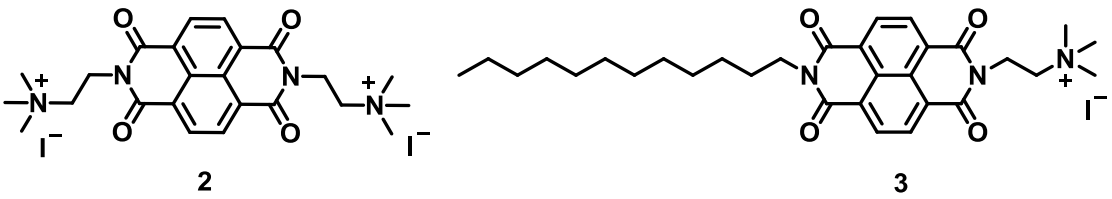

Scheme S2: Chemical structure of control molecules **2** and **3**.

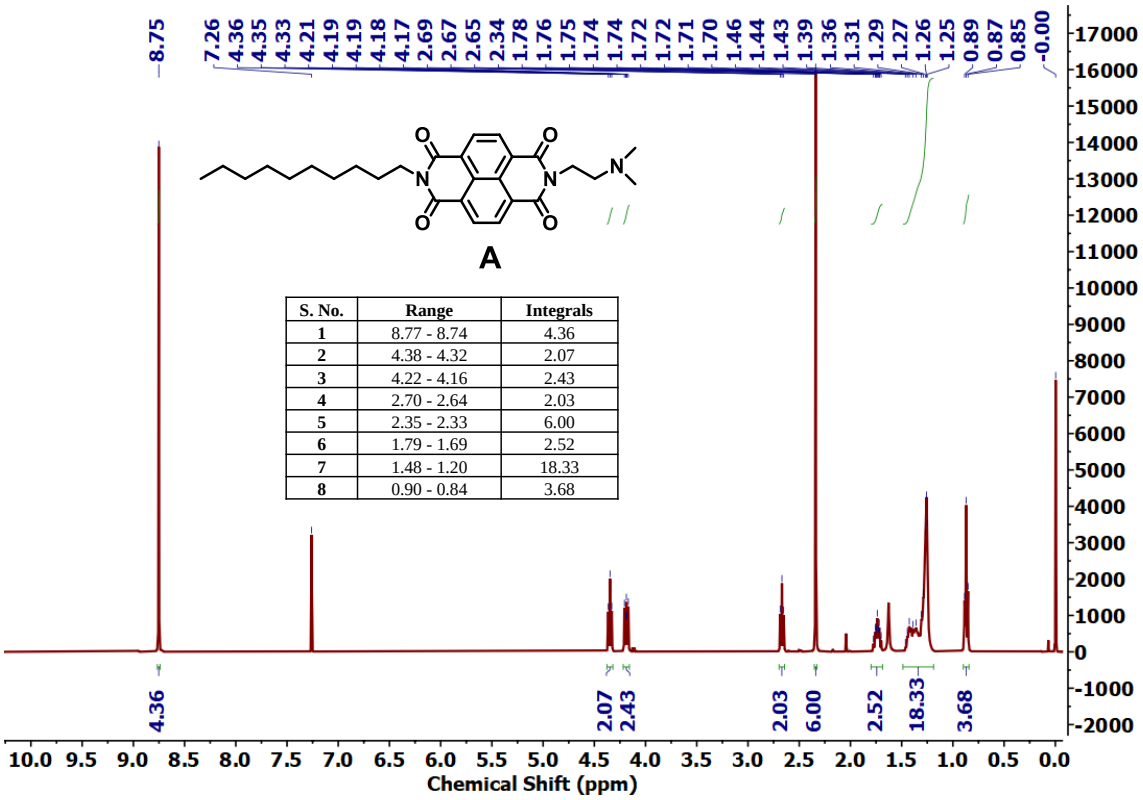

S. No.	Range	Integrals
1	8.77 - 8.74	4.36
2	4.38 - 4.32	2.07
3	4.22 - 4.16	2.43
4	2.70 - 2.64	2.03
5	2.35 - 2.33	6.00
6	1.79 - 1.69	2.52
7	1.48 - 1.20	18.33
8	0.90 - 0.84	3.68

Figure S1: ^{1}H NMR spectrum of NDI derivative **A** in $CDCl_3$ at 298 K.

The integration for the signal at 8.75 ppm is 4.37 instead of 4. This is due to the reason described with the synthesis procedure i.e. product A was ~92% pure. The 8% impurity was due to both sides alkylated product i.e., C_{10}-NDI-C_{10}. This impurity is not reactive towards methyl iodide and soluble in toluene. So, it's easy to remove this in the next step workup. Therefore, we directly used this product for next step.

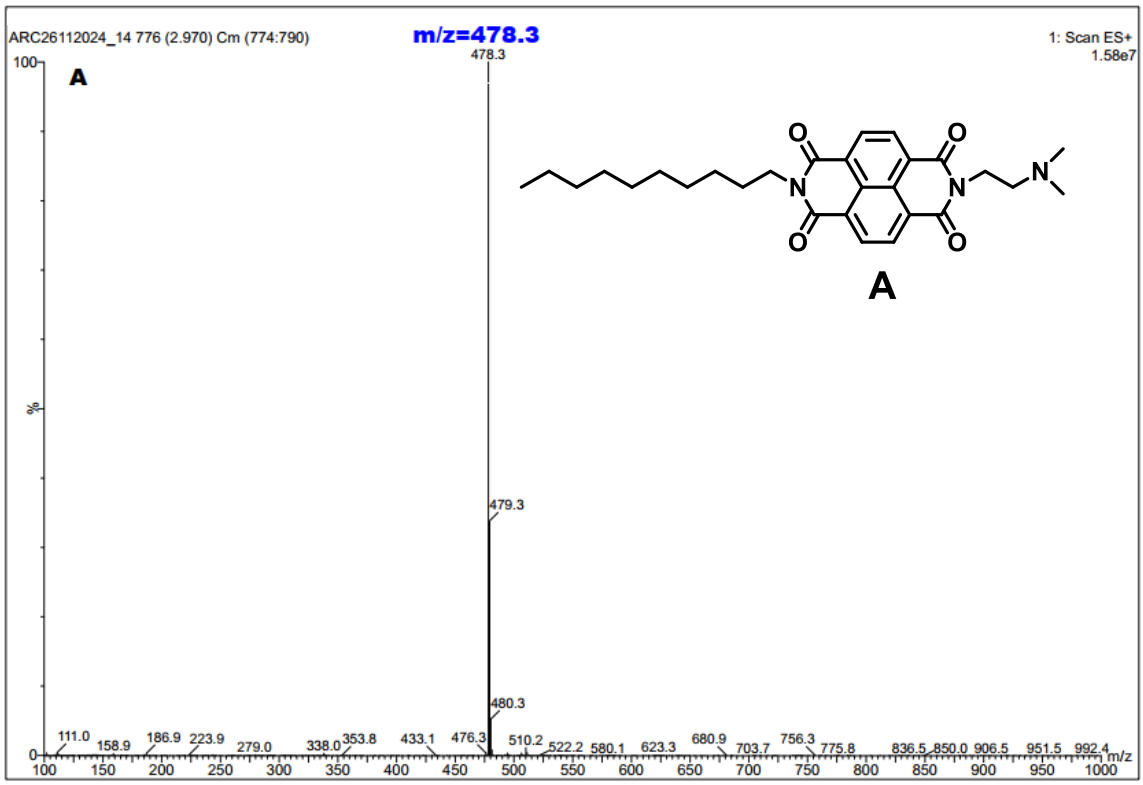

Figure S2: ESI-MS spectrum of **A**.

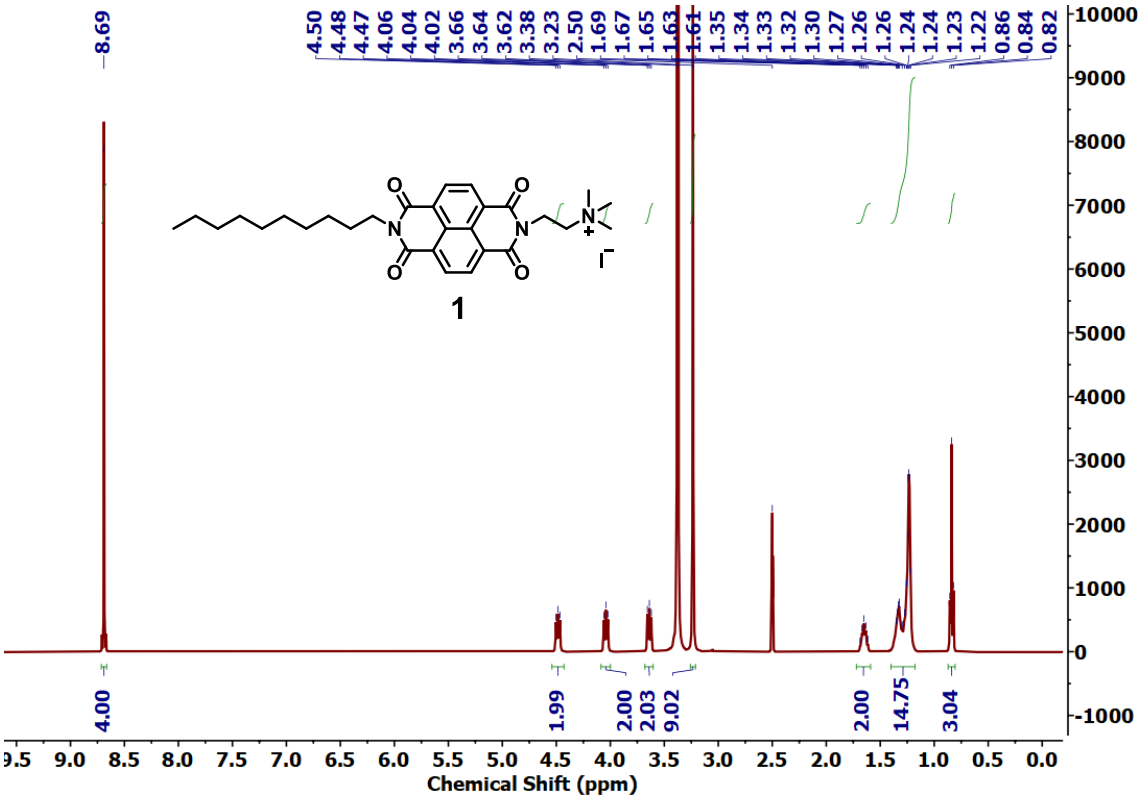

Figure S3: ^{1}H NMR spectrum of **1** in DMSO-d_6 at 298 K.

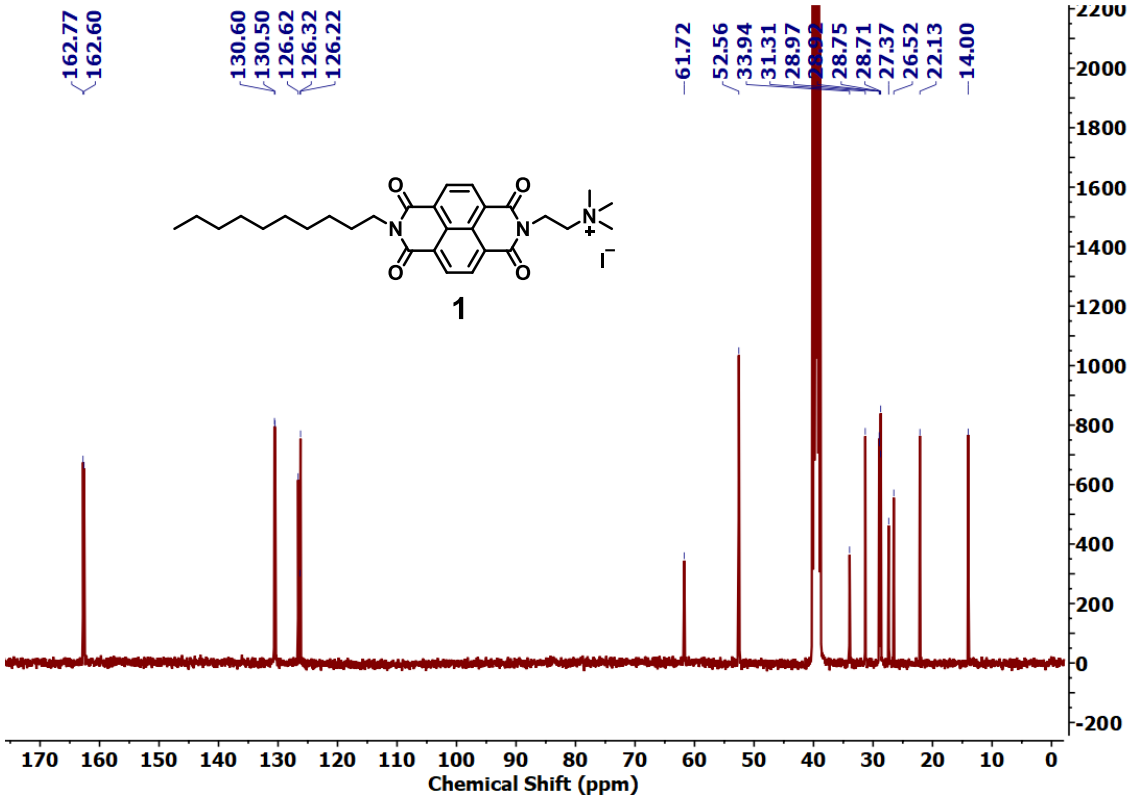

Figure S4: ^{13}C NMR spectrum of **1** in DMSO-d_6 at 298 K.

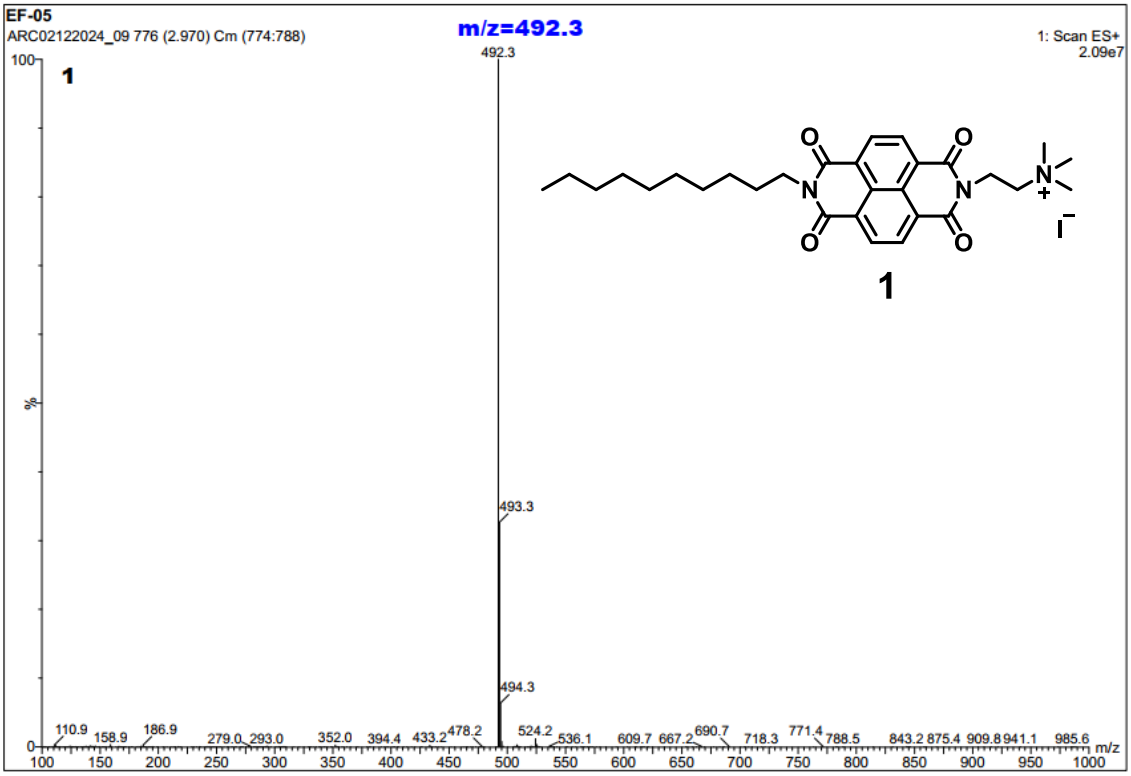

Figure S5: ESI-MS spectrum of **1**.

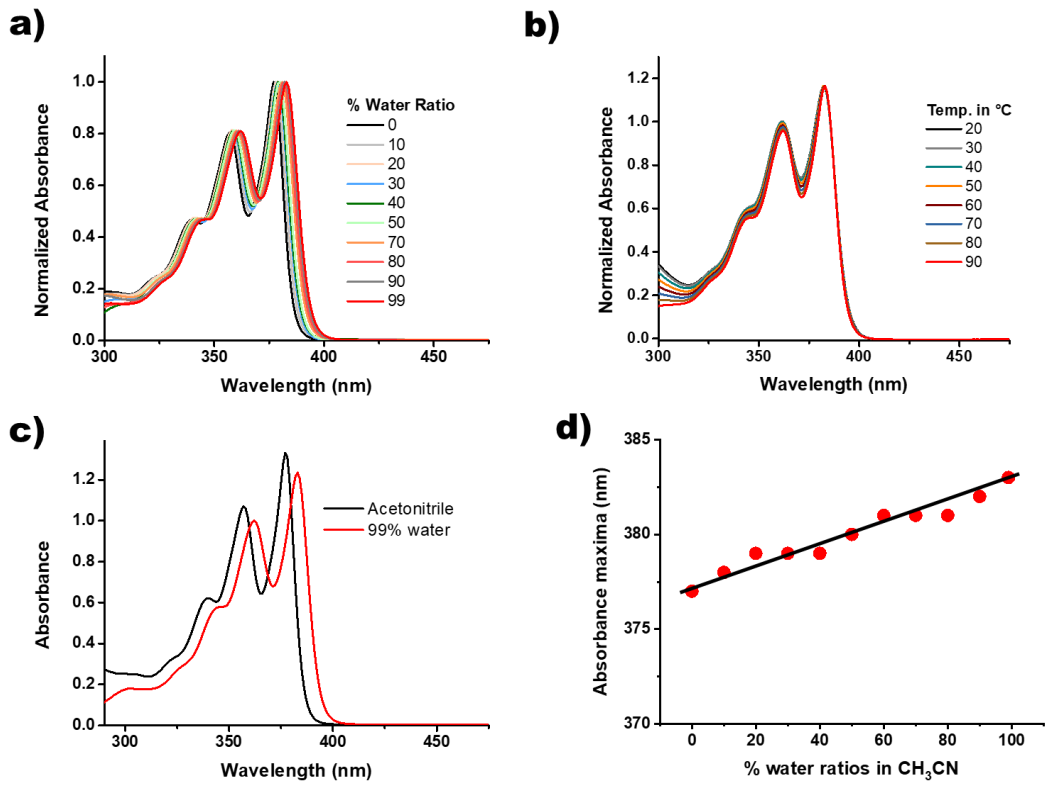

Figure S6: (a) Solvent dependent normalized UV-Vis absorption spectra of 50 μM concentration of **1**; (b) UV-Vis absorption spectra of **1** (50 μM) in 99% water-acetonitrile solvent composition at different temperatures ranging from 20-90°C; (c) UV-Vis absorption spectra in acetonitrile and 99% water showing solvent dependent absorbance shift and (d) a plot of absorbance λ_{max} vs % water ratios of **1** (50 μM) in acetonitrile obtained from a. The line is positioned to guide the eye.

The near linear shift of the absorbance maxima upon increasing water % indicates that the change is likely due to solvatochromic effect.

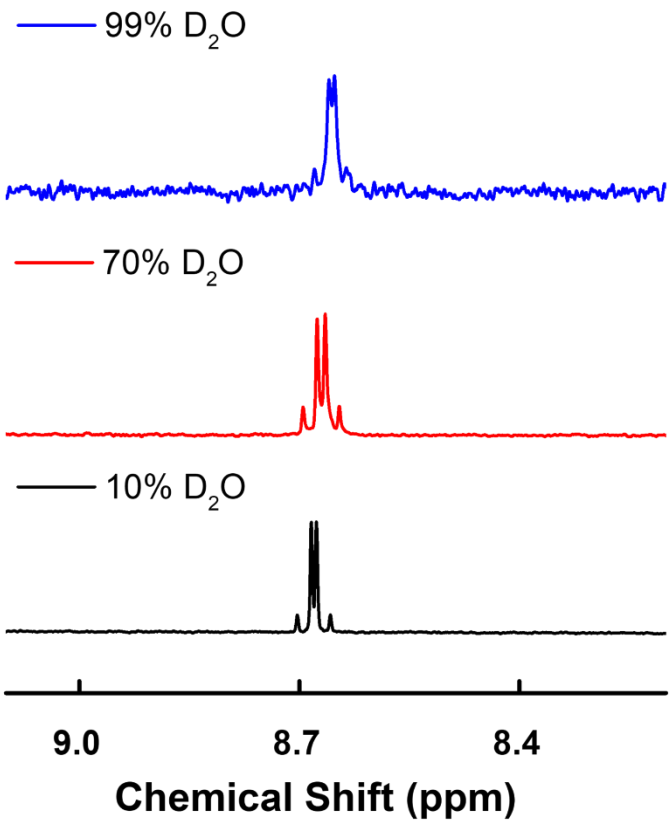

Figure S7: Proton NMR spectra of **1** (0.5 mM) in 10%, 70% and 99% D_2O in acetonitrile showing the monomeric nature.

The sharp aromatic peaks of the naphthalene core at δ 8.67 ppm with no signal broadening in different solvent compositions confirms the monomeric nature of **1**. A slight shift in the proton NMR peak positions in other water ratios compared to 10% D_2O sample can be because of the change in electronic environment due to different solvent compositions or just because of the NMR locking issue when a mixture of solvents is involved.

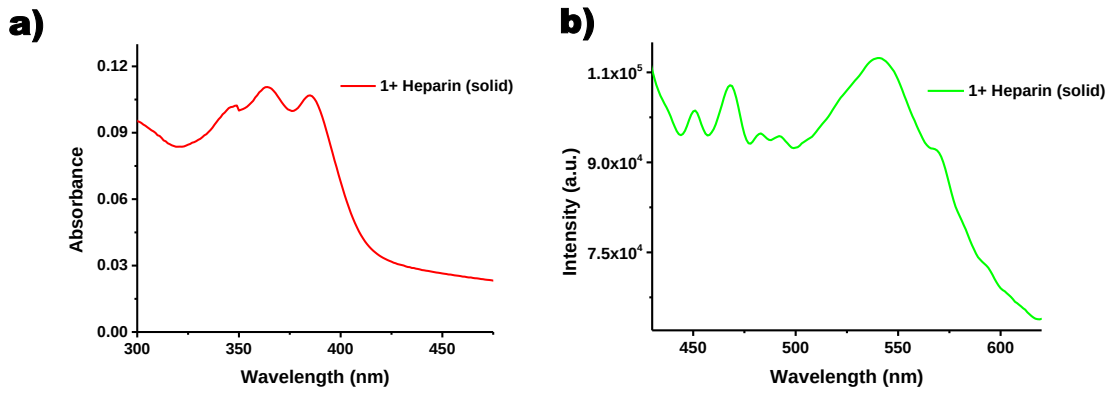

Figure S8: a) UV-Vis absorption and b) fluorescence spectra of dried sample (thin film) of **1** (200 µM) + heparin (51.6 µg/ml) in 70% water in acetonitrile solvent composition on a clean glass slide.

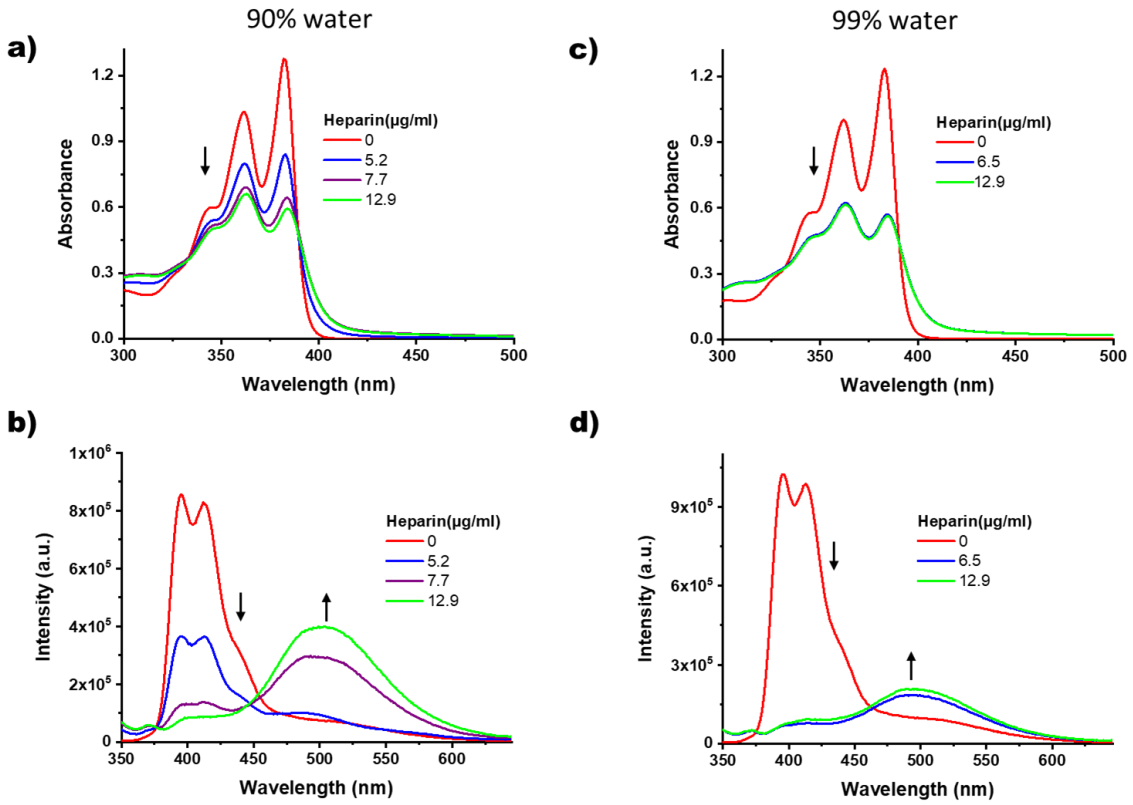

Figure S9: (a) UV-Vis absorption and (b) emission spectra of **1** (50 μM) with increasing amount of heparin in 90% water in acetonitrile solvent. The corresponding spectra for 99% water sample is shown in c and d.

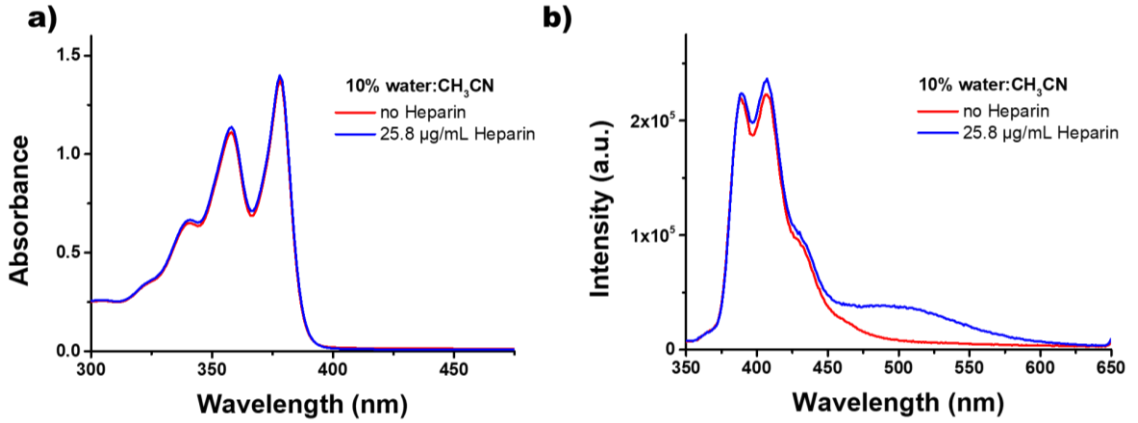

Figure S10: (a) UV-Vis absorption and (b) emission spectra of **1** (50 μM) with with 25.8 μg/ml heparin in 10% H_2O in acetonitrile solvent composition.

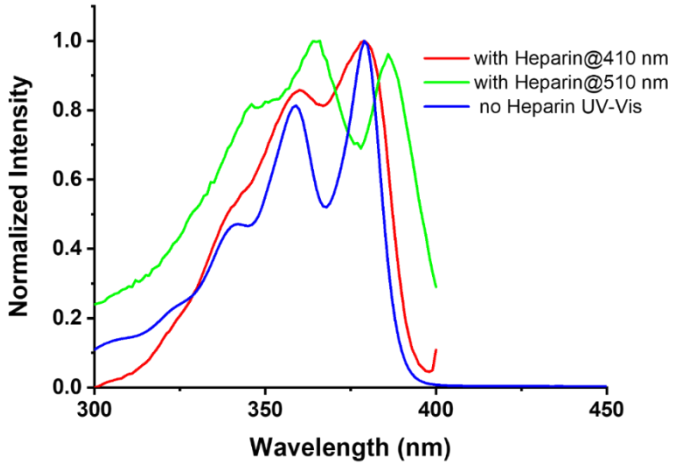

Figure S11: Excitation spectra of **1** upon binding with heparin in 40% water collected at λ_{em}= 510 nm, green line and λ_{em}= 410 nm, red line. These spectra were compared with the monomeric absorption spectra of **1** without heparin (blue line) in 40% H_2O. This data confirms the formation of static excimer in which the emission at 510 nm originates from the aggregated NDIs formed upon heparin addition.

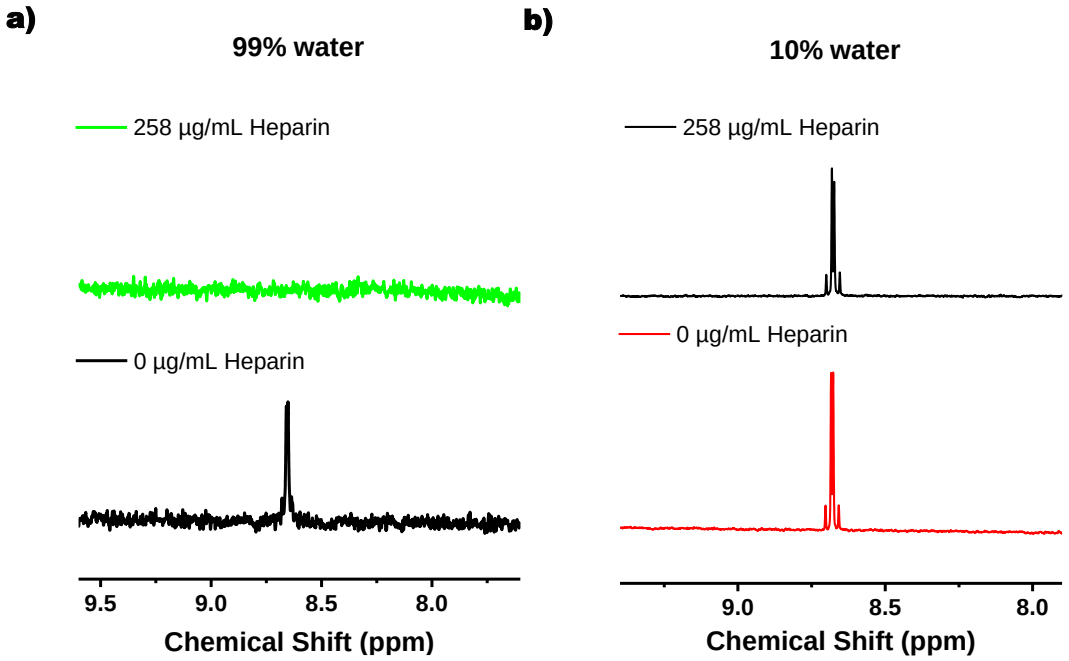

Figure S12: Proton NMR spectra of **1** (0.5 mM) in (a) 99% and (b) 10% water without and with 258 µg/mL heparin.

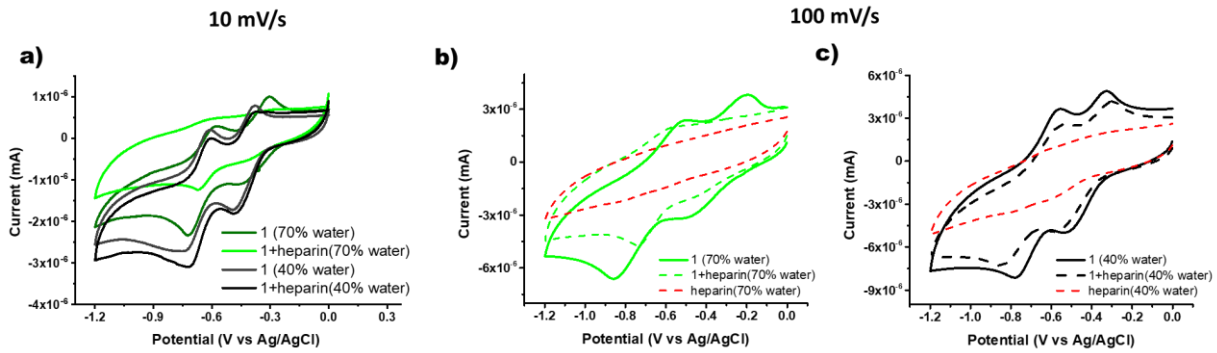

Figure S13: (a) Cyclic voltammogram (CV) of 100 μM concentration of **1** with and without heparin at a scan rate of 10mV/sec. CV profile of 100 μM concentration of **1** with and without heparin at a scan rate of 100 mV/sec for (b) 70% water and (c) 40% water.

Explanation: At fast scan speed of 100mV/sec, we can easily observe the reversible nature of the redox peak for NDI with heparin in 70% sample as seen in (b) (dashed green line). However, this was not very evident at slow scan rate of 10mV/sec.

What is evident from these experiments is that the 40% sample with and without heparin has very similar CV profile, in line with our spectroscopic results. However, binding of **1** to heparin in 70% water induces self-assembly. Therefore, the redox events in NDIs occur at different voltage compared to the sample without heparin as shown in (a and b).

Table S1: % Contribution of fluorescence lifetimes in 40 and 70% water in acetonitrile obtained with TCSPC measurement.

40% H_2O-acetonitrile					
Sample	**λ_{em}**	**τ_1**	**τ_2**	**% Contribution (τ_1)**	**% Contribution (τ_2)**
1	410 nm	0.18 ns	3.0 ns	75.6	24.4
1+Heparin	510 nm	1.3 ns	7.6 ns	38.7	61.3
70% H_2O-acetonitrile					
1	410 nm	0.14 ns	4.5 ns	93.8	6.2
1+Heparin	510 nm	2.2 ns	10 ns	21.4	78.6

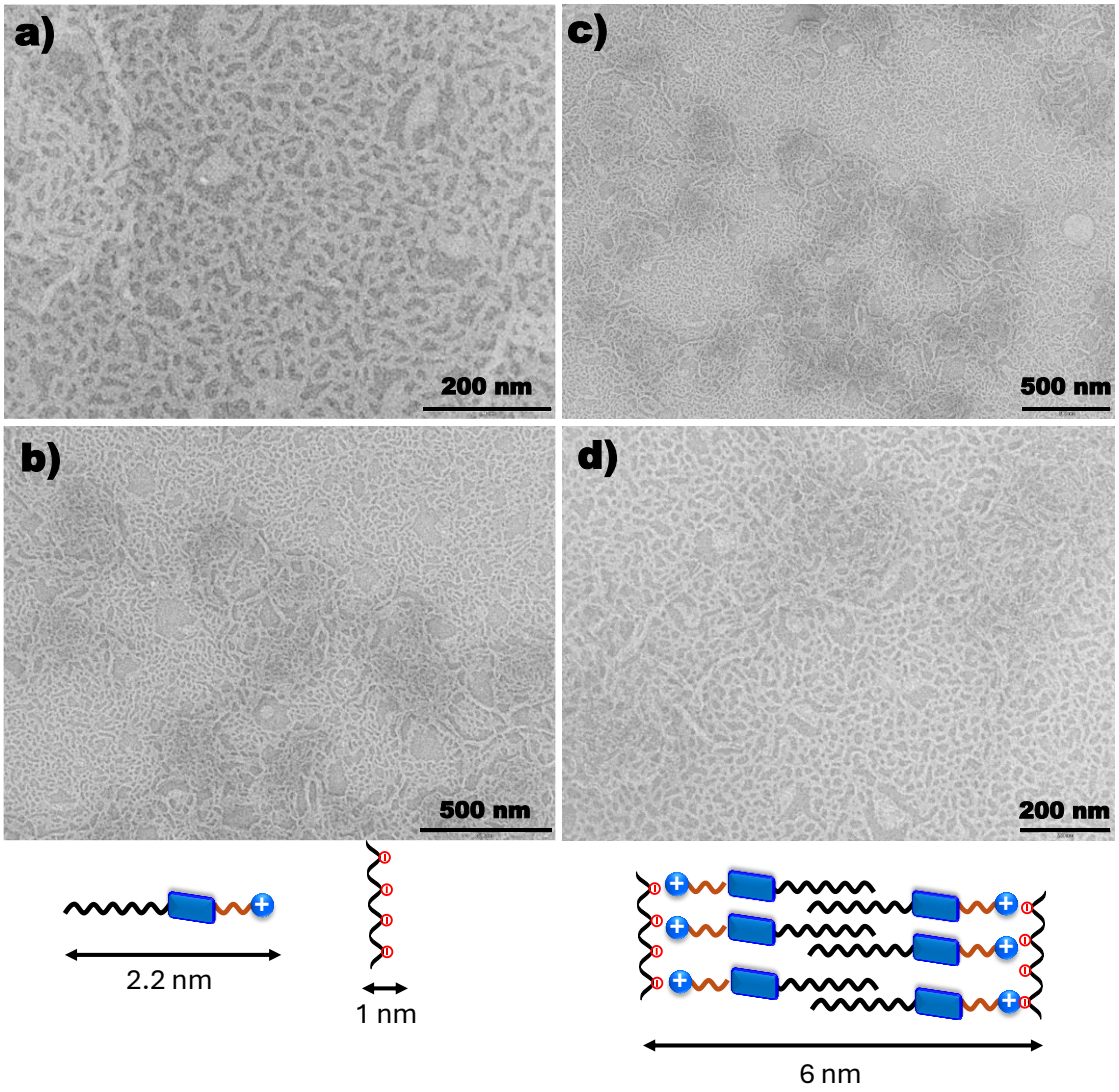

Figure S14: Additional TEM images of fibers formed by **1** (50 μM) upon 12.9 μg/ml heparin binding in 70% H_2O in acetonitrile. Below is the proposed molecular organization along with the expected dimensions.

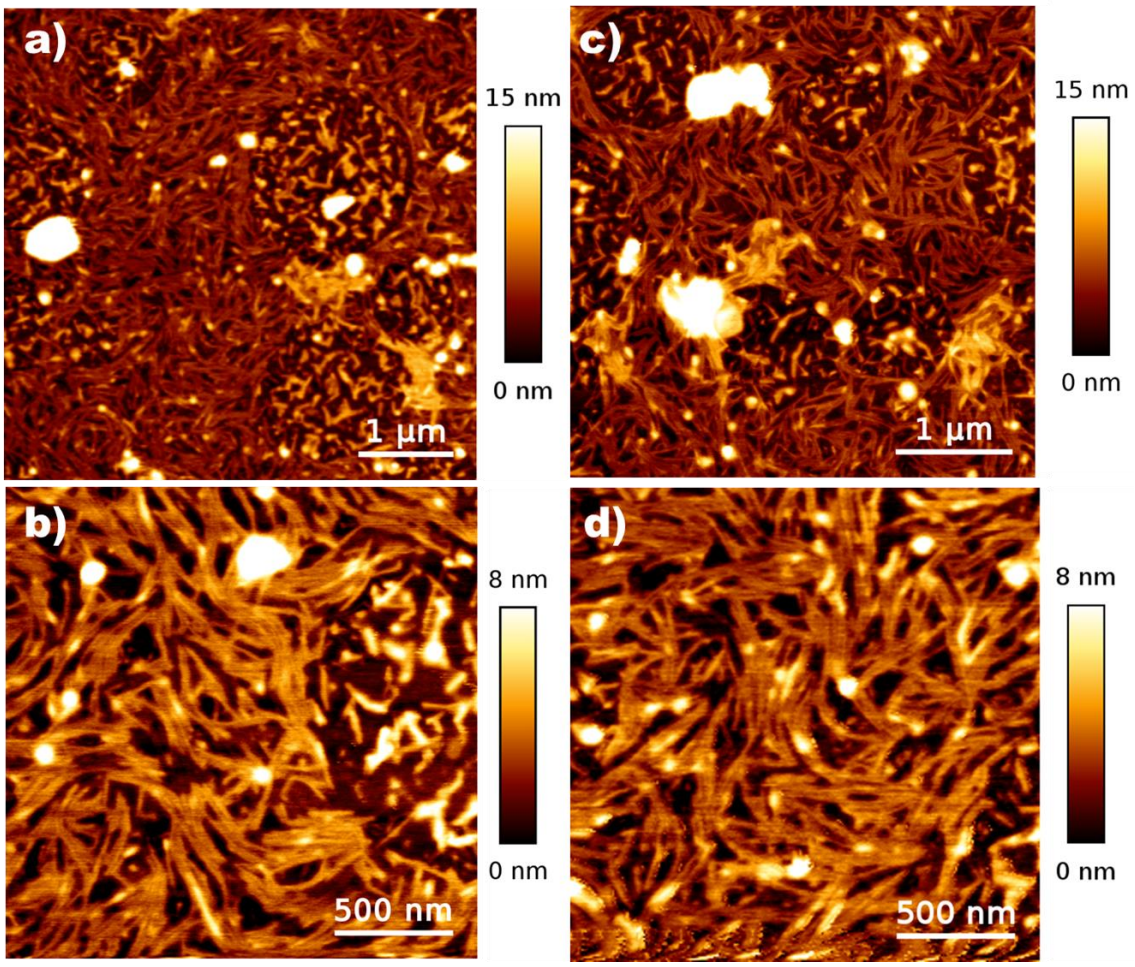

Figure S15: Additional AFM topographic images of **1** (50 µM) with 12.9 µg/ml heparin in 70% H_2O in acetonitrile. The sample was deposited on mica and dried. The imaging was performed in tapping mode over a 5 µm × 5 µm area (a), 2 µm × 2 µm area (b, d) and 4 µm × 4 µm area (c).

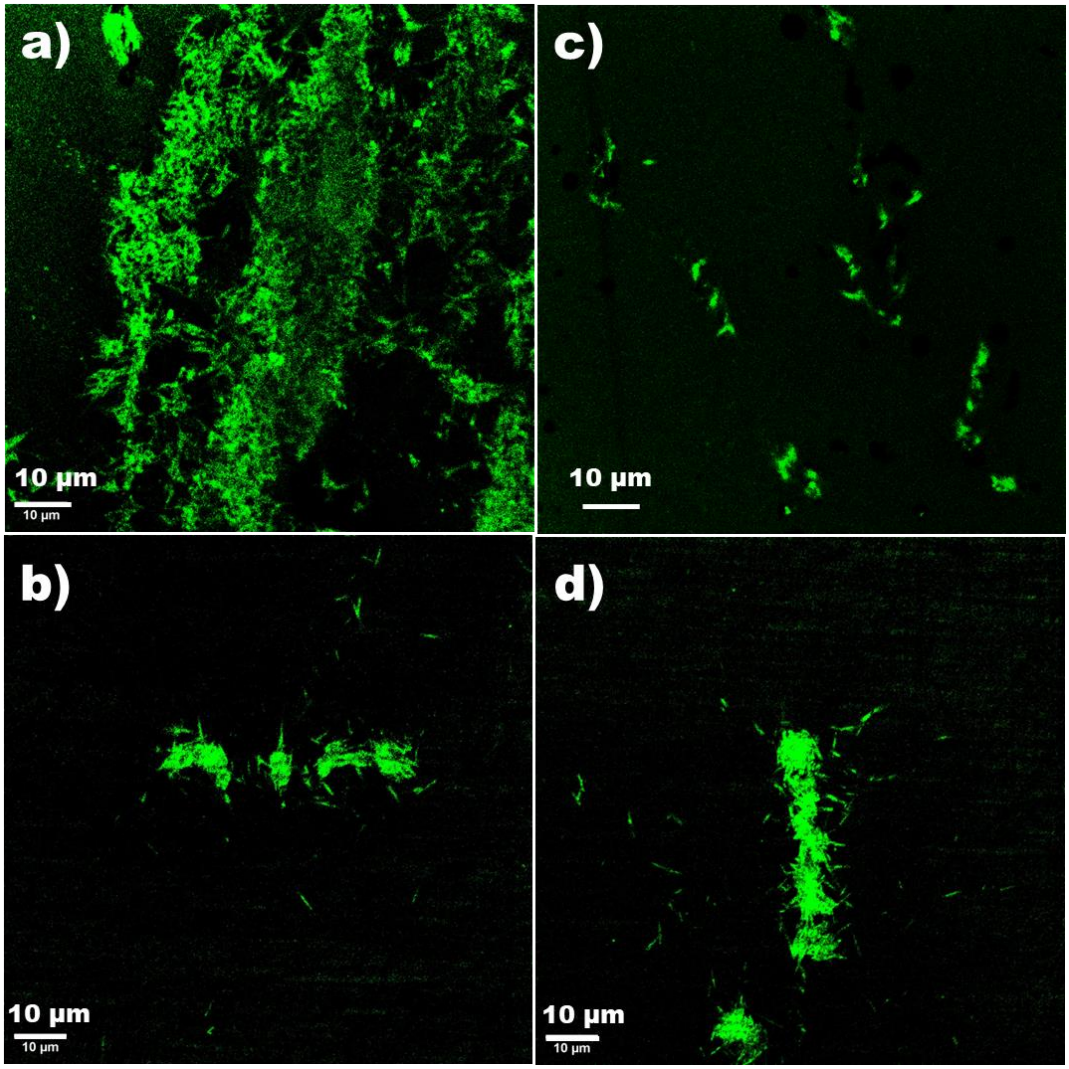

Figure S16: (a-d) Confocal Laser Scanning Microscopy (CLSM) images of the solution of **1** (200 µM) upon heparin binding showing the formation of nanofibers in 70% H_2O in acetonitrile solvent composition. Excitation at λ_{ex} = 405 nm and detection at the excimer band (500-700 nm) reveal strong green excimer emission along the fiber length, confirming the formation of fluorescent nanofibers of **1** with heparin in solution.

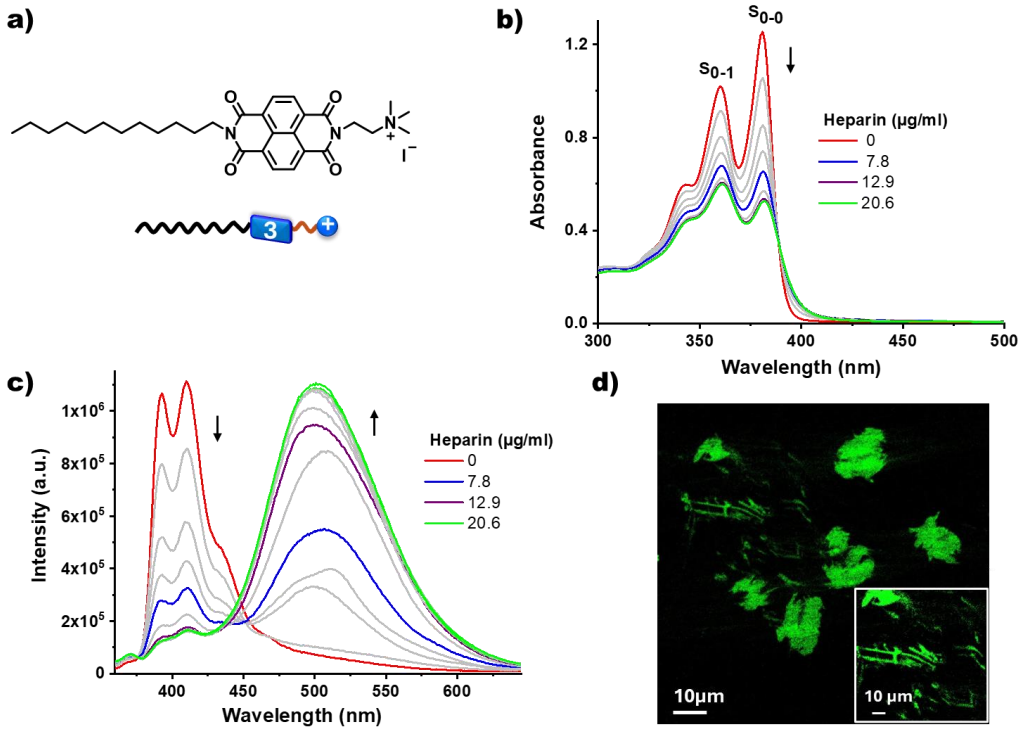

Figure S17: (a) Chemical structure and schematic representation of **3** containing carbon chain with 12 carbons; (b) Absorption and (c) emission spectra of **3** (50 μM) with varying concentrations of heparin showing heparin binding induced excimer emission in 70% H_2O in acetonitrile solvent composition and d) corresponding confocal image of **3** confirming the formation of fluorescent nanofibers of **3** with heparin in solution.

To probe the generalizability of the amphiphilic molecular design, we synthesized a new amphiphilic NDI derivative **3**. This molecule has longer carbon chain (12 carbon tail), which increases the hydrophobic character of the molecule. Interestingly, this molecule also showed very similar spectroscopic behaviour upon binding with heparin. Briefly, the UV-Vis spectra in 70% water showed that the presence of heparin resulted in the self-assembly of **3** (b). Furthermore, similar to **1**, binding of heparin to **3** also resulted in strong excimer emission at 510 nm (c). Furthermore, CLSM imaging also confirmed the formation of fluorescent nanofibers (d).

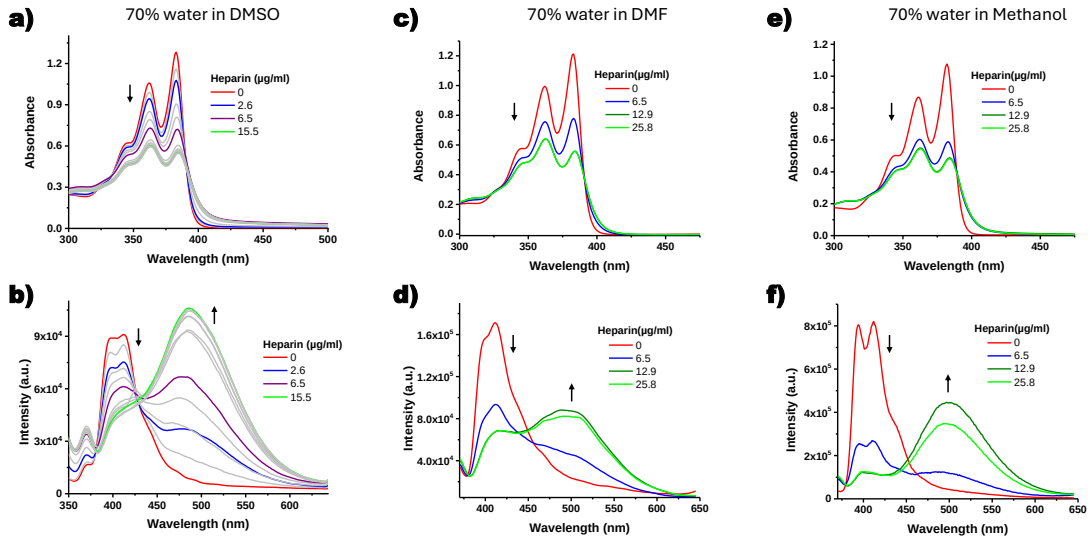

Figure S18: Absorption and emission spectra of **1** (50 μM) with increasing amount of heparin in a)-b) 70% water in DMSO; c)-d) 70% water in DMF; e)-f) 70% water in methanol solvent composition.

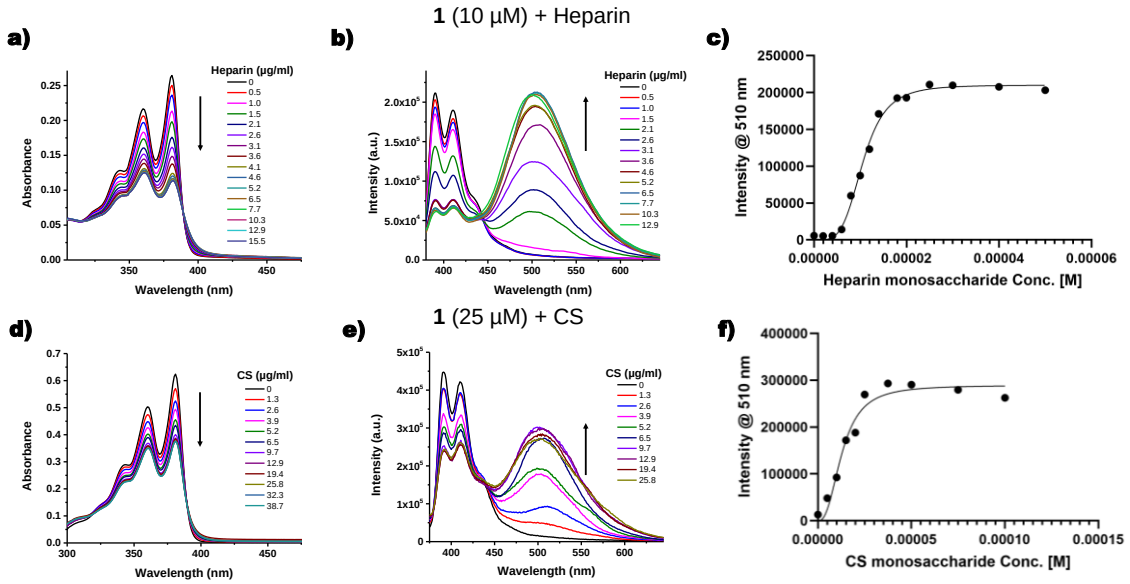

Figure S19: a) Absorption and b) emission spectra of **1** (10 μM) with increasing amount of heparin in 70% water in acetonitrile solvent composition. Similar graph for CS i.e. d) absorption and e) emission spectra of **1** (25 μM) with increasing amount of CS in 70% water in acetonitrile solvent composition. c) and f) are the respective plot of emission intensity at 510 nm against the heparin and CS concentration. The titration data in c) and f) were fitted using allosteric binding model of the GraphPad Prism to obtain the association constant. The solid line was obtained from the mathematical fitting using GraphPad Prism.

For obtaining association constant, the measurements were performed at lower concentration to obtain more reliable data.

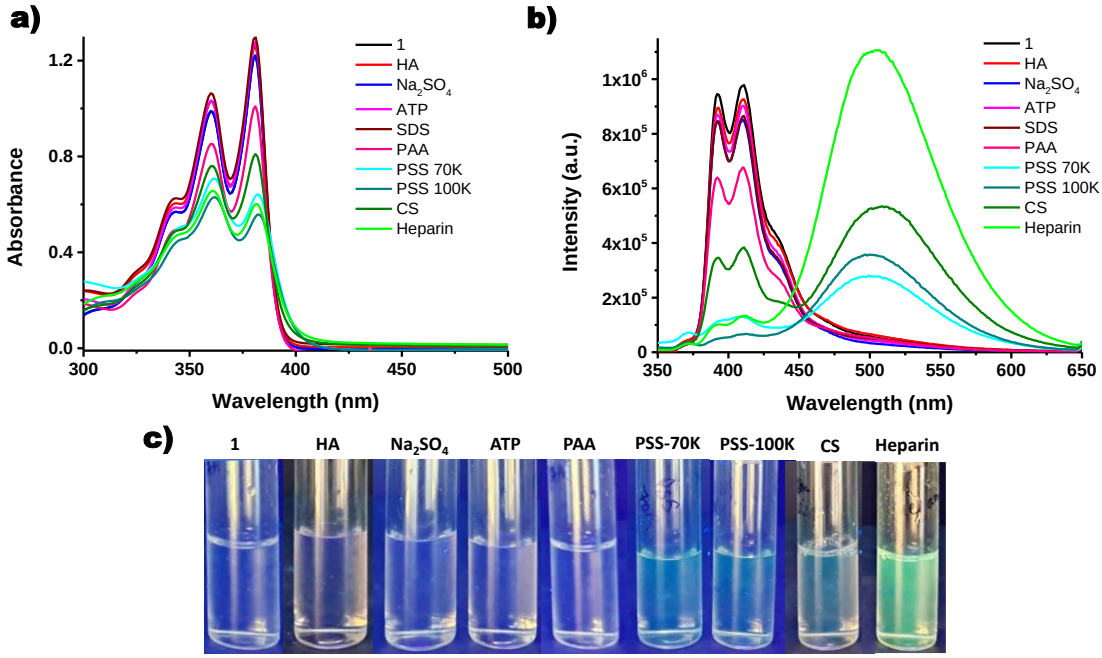

Figure S20: a) Absorption and b) emission spectra of **1** (50 µM) with 2 equivalents (w.r.t. monomer repeat unit) of different analytes in 70% H_2O in acetonitrile solvent composition; c) Photographs of **1** (50 µM) upon addition of different analytes: hyaluronic acid (HA), Na_2SO_4, adenosine triphosphate (ATP), sodium dodecyl sulphate (SDS), Polyacrylic acid (PAA), Poly(sodium 4-styrenesulphonate) (PSS-70K), Poly(sodium 4-styrenesulphonate) (PSS-100K), chondroitin sulphate (CS) and Heparin (2 molar equivalents w.r.t. their monomers) in 70% H_2O under 365 nm UV light.

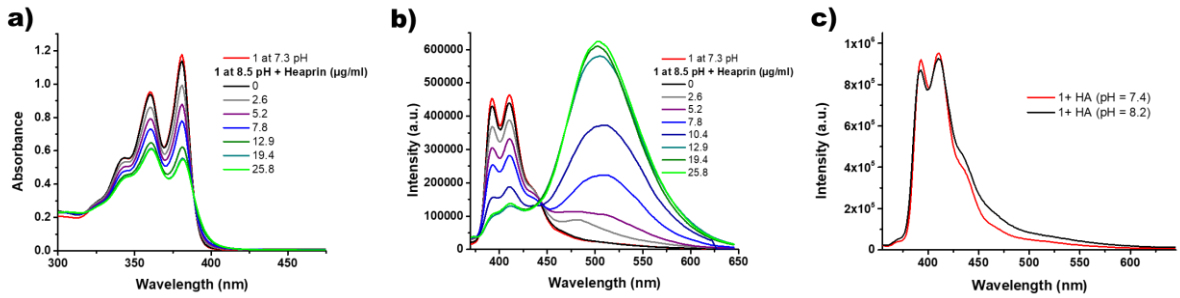

Figure S21: a) Absorption and b) emission spectra of **1** (50 µM) with increasing amount of heparin in 70% water in acetonitrile at 8.5 pH; c) emission spectra of **1** (50 µM) with 2 equivalents of hyaluronic acid (HA) in 70% water in acetonitrile solvent composition.

It shows that even at higher pH (8.5), heparin binds to **1** (figure S21a-b). But HA does not bind to **1** at the pH of Heparin bound **1** i.e. pH 8.2. This rules out any pH related influence in non-binding of HA to **1** (figure S21c).

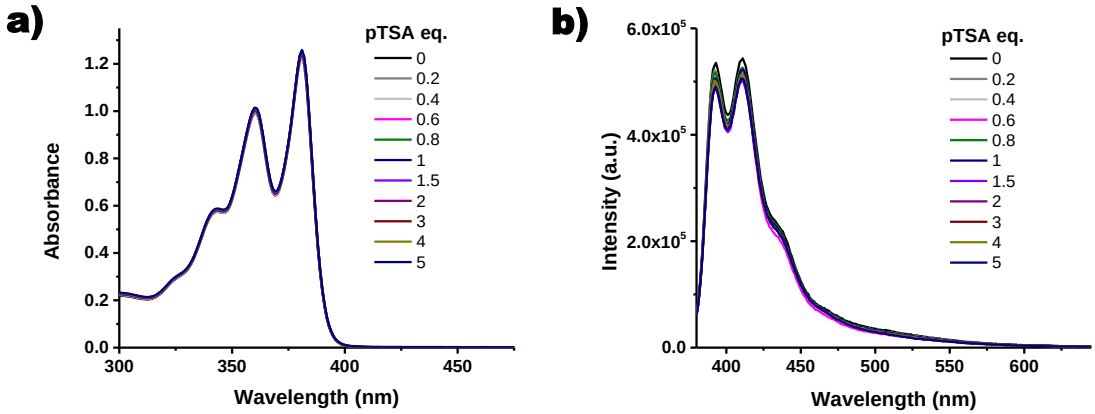

Figure S22: a) Absorption and b) emission spectra of **1** (50 μM) with different equivalents of p-Toluenesulfonic Acid (pTSA) in 70% H_2O in acetonitrile solvent composition.

p-toluenesulfonic acid (pTSA), a small, monovalent sulfonate does not bind to **1** to result in the excimer emission. This data confirms the role of multivalency in heparin and chondroitin sulphate binding to **1**.

4. References

1. a) S. Kuila, K. V. Rao, S. Garain, P. K. Samanta, S. Das, S. K. Pati, M. Eswaramoorthy and S. J. George, *Angew. Chem. Int. Ed.*, 2018, **57**, 17115-17119; b) K. Jalani, M. Kumar and S. J. George, *Chem. Commun.* , 2013, **49**, 5174-5176.